FITC Binding Site and *p*-Nitrophenyl Phosphatase Activity of the Kdp-ATPase of *Escherichia coli*†

Marc Bramkamp, Michael Gassel,‡ and Karlheinz Altendorf*

Abteilung Mikrobiologie, Fachbereich Biologie/Chemie, Universität Osnabrück, D-49069 Osnabrück, Germany

Received September 2, 2003; Revised Manuscript Received December 30, 2003

ABSTRACT: The KdpFABC complex of *Escherichia coli*, which belongs to the P-type ATPase family, has a unique structure, since catalytic activity (KdpB) and the capacity to transport potassium ions (KdpA) are located on different subunits. We found that fluorescein 5-isothiocyanate (FITC) inhibits ATPase activity, probably by covalently modifying lysine 395 in KdpB. In addition, we observed that the KdpFABC complex is able to hydrolyze *p*-nitrophenyl phosphate (pNPP) in a Mg^{2+}-dependent reaction. The pNPPase activity is inhibited by FITC and *o*-vanadate. Low concentrations of ATP (1−30 μM) stimulate the pNPPase activity, while concentrations of >500 μM are inhibitory. This behavior can be explained either by a regulatory ATP binding site, where ATP hydrolysis is required, or by proposing an interactive dimer. The notion that FITC inhibits pNPPase and ATPase activity supports the idea that the catalytic domain of KdpB is much more compact than other P-type ATPases, like Na^+,K^+-ATPase, H^+,K^+-ATPase, and Ca^{2+}-ATPase.

P-Type ATPases comprise a superfamily of enzymes involved in the transport of charged substrates across biological membranes. Members of the P-type ATPases are found in all kingdoms of life. This family of enzymes can be divided into different groups related to their substrate specificity (*1*, *67*). The heavy metal-transporting P-type ATPases belong to the type I class, while the mono- and divalent cation-transporting P-type ATPases were grouped into the type II class with different subgroups. This classification is mainly due to the size of the different domains and their organization. The Kdp-ATPases[1] found in a variety of prokaryotes, bacteria as well as archaea, share homologies with both groups and were therefore classified as type Ia (*1*). Besides several heavy metal-transporting ATPases, the Kdp-ATPase (KdpFABC complex) of *Escherichia coli* is the best studied bacterial P-type ATPase. This complex, synthesized under potassium starvation or high osmolality in the medium, is an emergency system that transports potassium ions with a remarkably high affinity ($K_m = 2$ μM) but moderate rates ($v_{max} = 150$ μmol g^{-1} min^{-1}) (*2*). The expression of the *kdpFABC* operon is under the control of the KdpD−KdpE two-component system (*3*−*5*). The KdpFABC complex is the only member of the large family of P-type ATPases where the catalysis of ATP, and hence the phosphorylation, and the binding and transport of the substrate occur on different subunits. The membrane-bound enzyme consists of four subunits (*6*, *7*). The largest subunit, KdpB (72 kDa), shares with other members of the family all conserved regions of a classical P-type ATPase. KdpA (59 kDa) is responsible for potassium binding and transport and is homologous with potassium channels (*8*, *9*). KdpC (21 kDa) might be involved in the assembly of the complex (*10*), and the small hydrophobic peptide, KdpF (3 kDa), was shown to stabilize the complex at least *in vitro* (*7*).

The transport process of P-type ATPases is driven by ATP hydrolysis in a reaction cycle that includes the transition of the enzyme from the E1 to the E2 conformation. The distinctive feature of P-type ATPases is the formation of a phosphoenzyme as an intermediate. The phosphorylation site is a conserved aspartate residue, which is located in a highly conserved DKTGT motif. All P-type ATPases share at least eight regions of homology first described by Serrano (*11*). These domains are believed to play essential roles in catalysis. Extensive studies on the biochemistry and structure−function relationship have been performed in the past several years, especially on the eukaryotic Na^+,K^+-ATPase and the Ca^{2+}-ATPase. Recently, the structures of the Ca^{2+}-ATPase (SERCA pump) at 2.6 Å resolution (E1 state) (*12*) and at 3.1 Å resolution [E2(TG) state] (*13*) were published. These first high-resolution structures of a P-type ATPase allow a first glimpse into the molecular architecture of P-type ATPases and confirm the modular character of this class of enzymes. The most prominent module is the phosphorylation domain, the architecture of which represents a classical Rossman fold. This motif is found in a variety of enzymes, recently grouped together into the HAD superfamily of enzymes, named after the L-2 haloacid dehalogenase (*14*). Since structural similarity exists between the different members of the P-type ATPase family, the structure of the SERCA pump provides a unique opportunity to model other

† Support for this study was provided by the Deutsche Forschungsgemeinschaft (SFB 431 and SPP 1070) and the Fonds der Chemischen Industrie.

* To whom correspondence should be addressed: Abteilung Mikrobiologie, Fachbereich Biologie/Chemie, Universität Osnabrück, D-49069 Osnabrück, Germany. Telephone: +49(0)541-9692864. Fax: +49(0)-541-96912891. E-mail: altendorf@biologie.uni-osnabrueck.de.

‡ Current address: Division of Pathochemistry, German Cancer Research Center (DKFZ), Im Neuenheimer Feld 280, D-69120 Heidelberg, Germany.

[1] Abbreviations: AMP-PNP, 5′-adenylimidodiphosphate; FITC, fluorescein 5-isothiocyanate isomer I; Kdp-ATPase, potassium-dependent adenosine triphosphatase (EC 3.6.1.36); pNPP, *p*-nitrophenyl phosphate; PAGE, polyacrylamide gel electrophoresis.

10.1021/bi030198a CCC: $27.50
Published on Web 03/23/2004

P-type ATPases.

However, compared with eukaryotic P-type ATPases, only little is known about the biochemical features of prokaryotic representatives. For the KdpFABC complex, it was previously shown that FITC is a potent inhibitor of the ATPase activity, but the binding site was not identified (*15*). It is well-established for the Ca^{2+}-ATPase (*16*) and for the Na^+,K^+-ATPase (*17*) that FITC binds in or near the ATP binding site. Therefore, FITC binding is often used as a tool for measuring effects related to this high-affinity ATP site (*18*−*23*). Sequence comparisons revealed that the KGSVD motif in the large cytoplasmic loop of KdpB is homologous to the KGAPE motif of other P-type ATPases and might therefore constitute the binding site for FITC. KdpB shares this motif with members of the type II−V classes of P-type ATPases.

In this report, we provide evidence that the conserved lysine residue in the KGSVD motif of the nucleotide-binding domain is the FITC binding site. Furthermore, we report for the first time that the KdpFABC complex exhibits pNPPase activity, which is a common feature of other enzymes of the same class.

EXPERIMENTAL PROCEDURES

Materials. All chemicals were analytical grade. All nucleotides and FITC were purchased from Sigma. pNPP was from ICN Biomedical Research Products. Protein molecular mass standards were purchased from NOVEX.

Bacterial Strains and Plasmids. E. coli strain TKW3205 (Δ*kdpFABC5*, Δ*atp*, *thi*, *rha*, *lacZ*, *nagA*, *trkA405 trkD1*) (*24*) was transformed with plasmid pSR4 (*25*) carrying the wild-type *kdpFABC* operon under the control of its natural promoter. The resulting transformants were grown in minimal medium containing 0.5 mM K^+ and 50 μg/mL ampicillin as described by Siebers and Altendorf (*26*).

Protein Purification. The KdpFABC complex was prepared as described by Siebers *et al*. (*27*). The final elution fraction from the TSK AF-Red affinity column contained 50 mM Tris-HCl (pH 7.5), 20 mM $MgCl_2$, 10% (v/v) glycerol, 750 mM NH_4Cl, and 0.2% (v/v) aminoxid. The protein-containing fractions were pooled, dialyzed against 50 mM Hepes-Tris (pH 7.5) and 0.035% (v/v) aminoxid, further treated as described in ref *28*, concentrated in an amicon cell, and stored in liquid nitrogen until they were used.

Phosphatase Activity. The phosphatase activity of the purified KdpFABC complex was measured in microtiter plates at 37 °C using a total reaction volume of 100 μL containing 20 mM Hepes-Tris (pH 7.8), 15 mM $MgCl_2$, and 50 μg/mL protein. After preincubation for 5 min at 37 °C, the reaction was started by adding 15 mM pNPP and stopped after 15 min with 0.1 M NaOH. The absorbance of the reaction product *p*-nitrophenolate was measured immediately at 410 nm, calibrating the microplate reader with water to give true extinction values. The total amount of released *p*-nitrophenolate was calculated using an extinction coefficient (ϵ) of 18.5×10^{-3} M^{-1} cm^{-1} or a *p*-nitrophenol standard curve. Each data point was an average of duplicate measurements. As controls, duplicates of the nonenzyme control were subtracted from each data point. The effect of nucleotides (1 min), ions, or inhibitors (5 min) was determined after preincubation at 37 °C for the indicated amount of time.

FITC Modification. Modification of the KdpFABC complex with FITC was carried out for 30 min at 37 °C in the dark (black microreaction tubes) in buffer containing 25 mM Tris-HCl (pH 9.2), 150 mM choline chloride, 12.5 mM histidine, and 1 mM $MgCl_2$ using an FITC concentration of 15 μM, unless stated otherwise. FITC was dissolved in dimethyl sulfoxide as a 10 mM stock solution prepared freshly before being used. To test the influence of nucleotides, the enzyme was preincubated with the corresponding nucleotide (5 mM) for 5 min at room temperature.

The FITC-labeled KdpFABC complex used for time course experiments was incubated with various FITC concentrations as described above. To remove unbound FITC, the samples were purified using NAP-5 columns (Amersham Pharmacia Bioscience, Freiburg, Germany) equilibrated with 50 mM Tris-HCl (pH 8.0), 10 mM $MgCl_2$, and 0.2% aminoxide. To check for residual free dye, SDS−PAGE was performed, and the gels were examined under UV light for FITC fluorescence. The actual labeling ratio was determined spectrophotometrically by using the molar extinction coefficient for FITC at 495 nm ($\epsilon = 68\,000$ M^{-1} cm^{-1}) and by determining the protein concentration using the BCA assay from Pierce.

CNBr Cleavage and Amino Acid Sequencing. For cleavage with cyanogen bromide, Coomassie blue-stained protein bands of KdpB were cut from an SDS−polyacrylamide gel and shaken overnight with 0.75 M CNBr dissolved in 80% (v/v) formic acid. After removal of CNBr by washing with 80% formic acid, evaporation, and neutralization, the peptides were separated by SDS−PAGE, transferred onto a polyvinylidenefluoride membrane, and stained with amido black. Peptide bands were cut out, and N-terminal microsequencing of protein fragments was carried out as described previously (*29*) with modifications described in ref *30* using an Applied Biosystems A473a protein sequencer.

Assays. Protein concentrations were determined by using the BCA assay from Pierce using bovine serum albumin as a standard. For protein samples containing detergent, like aminoxid, the method of Hartree (*31*) was used. The ATPase activity was determined after preincubation of the purified KdpFABC complex with different effectors using the automatic assay of Arnold *et al*. (*32*) or applying the microtiter assay described by Henkel *et al*. (*68*) with the modifications described by Altendorf *et al*. (*69*). Separation of proteins was achieved by SDS−PAGE according to the method of Laemmli (*33*) using a standard polyacrylamide concentration of 11% (w/v). The gels were stained with silver according to the procedure of Blum (*34*) or with Coomassie brilliant blue G250 (*35*).

RESULTS

Modification of the KdpFABC Complex with FITC. For other P-type ATPases, like Na^+,K^+-ATPase (*36*) and Ca^{2+}-ATPase (*18*), it was shown that incubation with stoichiometric amounts of FITC leads to complete inactivation of ATP hydrolysis. The conserved lysine residues (K501 and K515) in the Na^+,K^+-pump and Ca^{2+}-ATPase, respectively, were found to be the modified residues (*16*, *37*). These lysine residues belong to a conserved KGAPE motif that is found

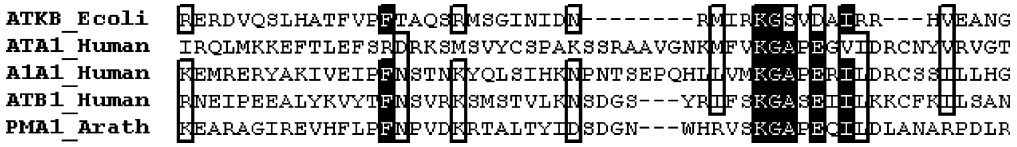

FIGURE 1: Alignment of the KGAPE motifs of different P-type ATPases. Chosen were ATPases representing different subgroups according to the nomenclature of Axelsen and Palmgren (*1*). Abbreviations: ATKB_ECOLI, potassium-transporting ATPase B chain of *E. coli* (EC 3.6.3.12); ATA1_HUMAN, sarcoplasmic/endoplasmic reticulum calcium ATPase 1 (EC 3.6.3.8, SERCA1) of *Homo sapiens*; A1A1_HUMAN, sodium/potassium-transporting ATPase α-1 chain precursor (EC 3.6.3.9) of *H. sapiens*; ATB1_Human, plasma membrane calcium-transporting ATPase 1 (EC 3.6.3.8, PMCA1) of *H. sapiens*; PMA1_ARATH, plasma membrane proton pump (EC 3.6.3.6) of *Arabidopsis thaliana*. Sequence information is derived from Swiss-Prot. The alignment was constructed using ClustalW with the default setting and edited using BioEdit. Conserved residues are on a black background, and similar residues are boxed.

FIGURE 2: CNBr cleavage of the FITC-modified KdpB subunit. After being labeled with 15 μM FITC, the subunits of the KdpFABC complex were separated by SDS−PAGE. KdpB was digested with CNBr; the generated fragments were separated by SDS−PAGE, transferred onto a polyvenylidene fluoride membrane, and examined under UV light. The amino acid sequence of the two labeled peptides is given. The KGSVD motif is shown in bold letters, and other lysine residues are in italics.

in many P-type ATPases (for a review, see ref *1*). The KdpB subunit of *E. coli* shares this motif, but it is important to mention that only the first two amino acids of the 395-KGSVD-399 sequence are conserved (see Figure 1). Therefore, it was unclear whether the FITC molecule exclusively modifies lysine 395 in KdpB. Previous labeling studies showed that FITC binds to all three large Kdp subunits (A. Siebers and K. Altendorf, unpublished results). However, we could demonstrate that the binding of FITC to subunits KdpA and KdpC is unspecific, probably due to hydrophobic interactions between the fluorescent dye and the proteins. Addition of salts, like NaCl or choline chloride, to maintain a high ionic strength, prevented unspecific labeling. With 150 mM choline chloride in labeling buffer, only KdpB was modified by FITC (compare Figure 3). The FITC-labeled KdpB band was cleaved with CNBr, and after blotting had been carried out, two bands exhibited characteristic FITC fluorescence (Figure 2). Amino acid sequencing revealed that lysine 395 was present in both peptides. The larger fragment resulted from cleavage after methionine 383 (see Figure 2 for the sequence). Sequencing of the smaller peptide showed that the cleavage site was located after methionine 392. Both peptides contain the KGSVD motif, making it likely that lysine 395 of KdpB is modified by FITC, although there are some other lysine residues in the C-terminal part of both peptides.

Influence of Nucleotides on FITC Modification. The fluorescent dye FITC binds predominantly in the high-affinity nucleotide-binding site of P-type ATPases to a conserved lysine residue (*17*, *18*, *36*−*38*). However, replacement of this conserved lysine residue in the plasma membrane Ca^{2+}-ATPase did not result in a loss of FITC binding (*39*). For the Na^+,K^+-ATPase, it was also shown that any of several lysine residues can react with FITC, leading to inhibition of ion-stimulated ATPase activity (*40*). Nevertheless, the structures of the Ca^{2+}-ATPase (*12*) and of the N-domain of the Na^+,K^+-ATPase (*41*) revealed that the conserved lysine residue, to which FITC predominantly binds in the wild-type enzyme, is located in the depth of the nucleotide-binding domain, making contact with the adenosine moiety of ATP. Consequently, FITC modification of the KdpB subunit could be prevented by preincubation with adenine nucleotides (see Figure 3). Interestingly, ATP, ADP, and AMP protected the solubilized enzyme. However, there was always a very small but distinct difference between ATP on the one side and ADP and AMP on the other. In the case of the Na^+,K^+-ATPase (*42*) and the Ca^{2+}-ATPase (*16*, *43*), only ATP and ADP, but not AMP, mediated protection against FITC modification. Other nucleotides such as GTP or ITP had no effect. The SDS-denatured enzyme was found to be no longer modified by FITC, indicating the necessity of a properly folded nucleotide-binding domain for FITC binding (compare with Figure 3). Similar protective effects were previously reported for the Na^+,K^+-ATPase (*42*). As can be seen in Figure 3, degradation products of KdpB (KdpB*) are also labeled. It was previously reported that FITC is a potent inhibitor of the ATPase activity of the KdpFABC complex (*26*). This irreversible inhibition was obviously pH-dependent. We determined half-maximal ($K_{0.5}$) inhibition of the ATPase activity at pH 9.2 with 3 μM FITC, which is largely shifted to a $K_{0.5}$ of 32 μM at pH 7.5.

p-Nitrophenyl Phosphatase Activity of the Kdp-ATPase. Eukaryotic P-type ATPases lack a stringent substrate specificity for both substrate hydrolysis and phosphorylation. Compounds such as acyl phosphate, carbamyl phosphate, *p*-nitrophenyl phosphate, and purine nucleotides were shown to be suitable phosphate donors for the Ca^{2+}-ATPase, for example (*44*−*48*). For the Kdp-ATPase, for the first time, we could measure the Mg^{2+}-dependent pNPPase activity with the purified enzyme. Mg^{2+} ions are essential for the pNPP hydrolysis, as is the case for all the other P-type ATPases. It was shown that Mg^{2+} plays a role in the coordination of the substrate into the binding pocket (*49*, *50*). The kinetics of hydrolysis follow a classical Michaelis−Menten scheme (see Figure 4). The K_m for the purified wild-type enzyme was 5.2 mM, and the v_{max} was 110 nmol mg^{-1} min^{-1}. The pH optimum of this reaction (pH 8.0, data not shown) was found to be in the same range as that determined for the ATPase activity (pH 7.8) (A. Siebers and K. Altendorf, unpublished results). In the case of the Na^+,K^+-pump (*51*), pNPPase is stimulated by potassium ions, and the KdpFABC complex has been proposed to have a similar reaction cycle (*52*). However, none of the ions that were tested, including

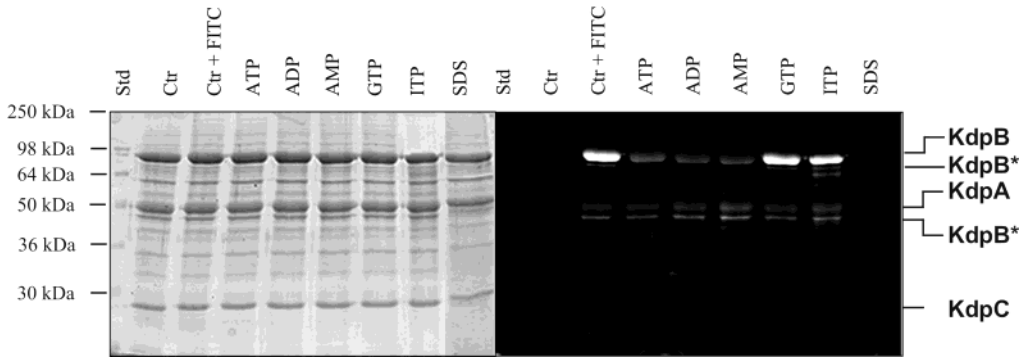

FIGURE 3: Influence of nucleotides on FITC modification of KdpB. The KdpFABC complex was incubated for 5 min with the indicated nucleotides (5 mM) and labeled with 15 μM FITC, and the proteins were separated by SDS−PAGE. Abbreviations: KdpB*, degradation product of KdpB; Std, molecular mass standard; Ctr, protein without FITC added; Ctr + FITC, protein incubated with FITC without added nucleotides; ATP, ADP, AMP, GTP, and ITP, enzyme complex incubated with the indicated nucleotide prior to FITC labeling; SDS, KdpFABC complex denatured with 1% (w/v) SDS prior to FITC addition. The left panel shows a Coomassie blue stain of the polyacrylamide gel, while the right panel shows the same gel under UV light before staining.

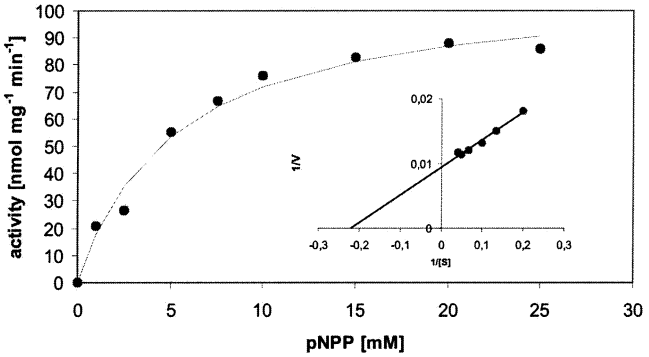

FIGURE 4: Hydrolysis of pNPP by the KdpFABC complex. Shown is a Michaelis−Menten diagram of the pNPP hydrolysis mediated by the Kdp-ATPase. The enzyme concentration was 50 μg/mL. The pNPP hydrolysis was assessed for 30 min and stopped with 100 μL of 0.1 M NaOH. The specific activity was calculated with a *p*-nitrophenol standard curve. All data points are mean values out of three independent experiments, and the mean values of three nonenzyme controls were subtracted. The buffer conditions were 50 mM Tris-HCl (pH 8.0), 10 mM $MgCl_2$, and 0.2% aminoxide. A double-reciprocal plot is shown in the inset.

potassium ions, had a stimulating effect on pNPP hydrolysis. In contrast, at concentrations of 50 mM, potassium, ammonium, and rubidium ions inhibited (45−50%) pNPP hydrolysis (data not shown). Addition of the same amount of sucrose had almost no effect (10% inhibition) on pNPP hydrolysis (data not shown), suggesting that osmolality effects can be ruled out.

Influence of o-Vanadate on ATPase and pNPPase Activity. The phosphate analogue *o*-vanadate was previously shown to inhibit the ATPase activity of the KdpFABC complex (*15*). A comparison of the inhibitory effect of *o*-vanadate on ATPase and pNPPase activity revealed that the inhibition kinetics of *o*-vanadate on ATP hydrolysis are different compared to those on pNPPase activity. The K_i values for the ATPase activity were determined to be 19.9 μM in the presence and 21.6 μM in the absence of potassium ions (1 mM). Like other P-type ATPases, the Kdp-ATPase exhibits nonlinear kinetics in a double-reciprocal plot of ATP hydrolysis, indicating non-Michaelis−Menten kinetics. The Michaelis−Menten plot of the ATP hydrolysis of the Kdp-ATPase is sigmoid (data not shown) with a corresponding Hill coefficient of 1.4, indicating allosteric or cooperative effects of the ATP-binding sites. The *o*-vanadate inhibition

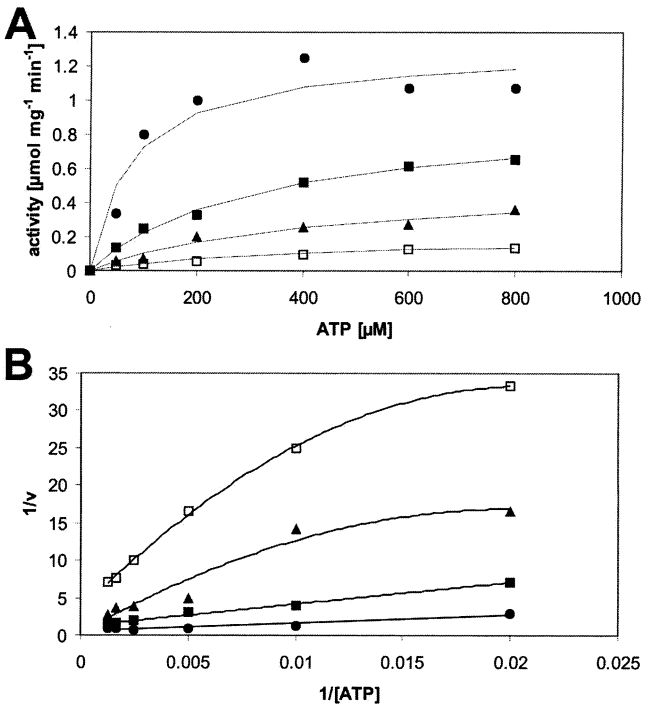

FIGURE 5: Inhibition kinetics of *o*-vanadate toward ATP hydrolysis of the KdpFABC complex. ATP hydrolysis by the KdpFABC complex was assessed at varying ATP concentrations. The enzyme was preincubated with the inhibitor for 5 min at 37 °C. The reaction was started by addition of ATP. A double-reciprocal plot is shown in panel B. The data were fitted using a second-order polynomial: (●) 0, (■) 1, (▲) 5, and (□) 20 μM *o*-vanadate.

of the ATPase activity follows obviously a more complex mechanism (for reasons of clarity, only the data in the absence of potassium ions are shown), as indicated by the nonlinear relation in the double-reciprocal plot in Figure 5B. The double-reciprocal plot was fitted with a second-order ratio of polynomials, suggesting the influence of at least two cooperative sites.

The *o*-vanadate inhibition of the pNPPase is not as complex (Figure 6A). A K_i value of 2.2 μM for the *o*-vanadate inhibition was determined. Figure 6B shows that the inhibition kinetics of the pNPP hydrolysis are competitive.

Influence of Adenine Nucleotides on pNPPase Activity. Previously, for the Na^+,K^+-ATPase, it was reported (*53*) that

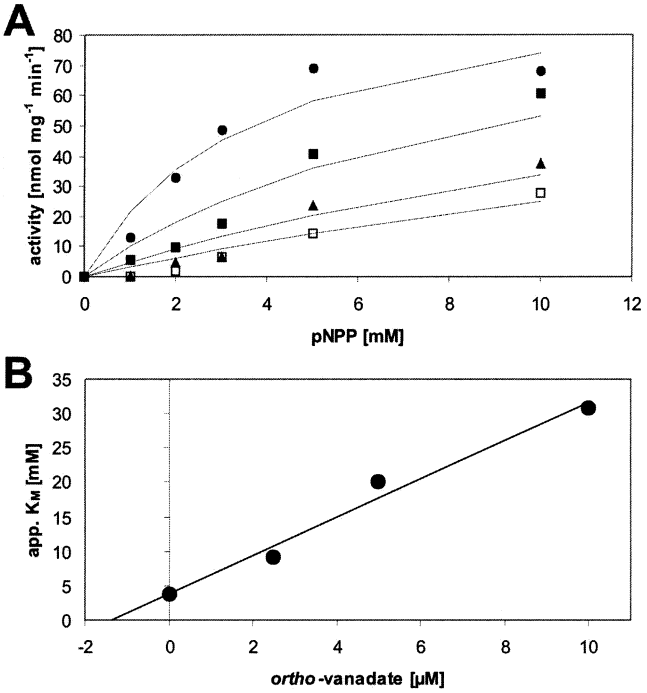

FIGURE 6: Inhibition kinetics of *o*-vanadate toward pNPP hydrolysis of the KdpFABC complex. (A) Classical Michaelis−Menten plot of *o*-vanadate inhibition of the pNPP hydrolysis. The enzyme (5 μg) was preincubated with the inhibitor for 5 min at 37 °C. The reaction was started by addition of pNPP: (●) 0, (■) 2.5, (▲) 5, (□) 10 μM *o*-vanadate. (B) Inhibition kinetics.

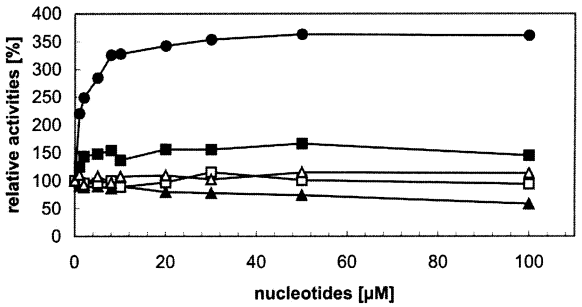

FIGURE 7: Effect of nucleotides on the pNPP hydrolysis of the KdpFABC complex. Prior to pNPP addition, the KdpFABC complex (5 μg) was incubated for 1 min with the different nucleotides in Hepes-Tris (pH 7.8) and 15 mM $MgCl_2$. The pNPPase reaction was started with 15 mM pNPP and stopped by addition of 0.1 M NaOH after 15 min. The activities are indicated as percent values with an activity of 71 μmol g^{-1} min^{-1} as the 100% value: (●) ATP, (■) ADP, (▲) AMP, (□) GTP, and (△) AMP-PNP.

low concentrations of ATP ($\leq$100 μM) stimulate the hydrolysis of pNPP while concentrations above 100 μM inhibit the reaction. In case of the sarcoplasmic reticulum Ca^{2+}-ATPase, the fluorescein derivatives eosin and erythrosin were able to stimulate pNPP hydrolysis, however, only in the presence of Ca^{2+} (*54*). The enhanced turnover was not due to a change in the apparent affinity for the substrate, but is indeed due to an acceleration of the turnover of the enzyme. The pNPP hydrolysis of the KdpFABC complex was shown to be stimulated 3.5-fold (see Figure 7) at ATP concentrations below 100 μM, reaching a maximum around 30 μM ATP, whereas inhibition of the pNPPase activity was observed at ATP concentrations above 500 μM. ADP had only a slight stimulatory effect, while other nucleotides such as AMP

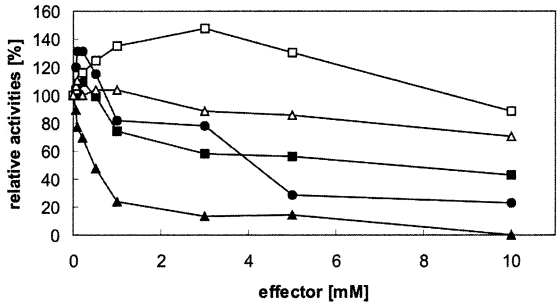

FIGURE 8: Effect of high effector concentrations on the pNPP hydrolysis of the KdpFABC complex. Prior to pNPP addition, the KdpFABC complex (5 μg) was incubated for 1 min with the different nucleotides (or P_i) in Hepes-Tris (pH 7.8) and 15 mM $MgCl_2$. The pNPPase reaction was started with 15 mM pNPP and stopped by addition of 0.1 M NaOH after 15 min. The activities are indicated as percent values with an activity of 71 μmol g^{-1} min^{-1} as the 100% value: (●) ATP, (■) ADP, (▲) AMP, (□) GTP, and (△) P_i.

showed no stimulation. Even the uncleavable ATP analogue AMP-PNP had no stimulatory effect, indicating that ATP hydrolysis is necessary for this stimulation. GTP was found to have a slight stimulatory effect at higher concentrations (3 mM) (see Figure 8). At millimolar concentrations, ATP, ADP, and inorganic phosphate exhibited an inhibitory effect with K_i values of 2.7 mM for ATP, 4.5 mM for ADP, and 25.6 mM for P_i. In contrast, a remarkable inhibition of the pNPPase activity by AMP with an observed K_i of ~500 μM was observed.

Effect of FITC on pNPPase Activity. Labeling with FITC has been extensively used as a tool to study effects related to the nucleotide-binding site of various P-type ATPases (*17*−*20*, *55*). It was reported that the covalently bound FITC inhibits ATP hydrolysis in a submillimolar range. However, it is well-known that FITC-labeled Ca^{2+}-ATPase, H^+-ATPase, and Na^+,K^+-ATPase are still able to hydrolyze pNPP. The inhibition by FITC is obviously based on the sterical hindrance of the nucleotide binding, while smaller substrates such as acyl phosphate and pNPP are still hydrolyzed. We studied the effect of the FITC modification of the KdpFABC complex on ATPase and pNPPase activity. In contrast to the larger eukaryotic ATPases mentioned above, we observed inhibitory kinetics of FITC for ATPase and pNPPase activity (Figure 9). FITC labeling was carried out at pH 9.2 as described in Experimental Procedures, and the same enzyme preparations were used for pNPPase and ATPase activity assays. To test whether one or more molecules of FITC were covalently bound to the Kdp-ATPase, the labeling ratio was determined spectrophotometrically using the molar extinction coefficient of FITC at 495 nm (pH 8.0). The labeling ratios were always close to 1 (0.7), indicating that only one molecule of FITC was bound to a KdpFABC complex. The kinetics of FITC inhibition were time- and concentration-dependent (Figure 9). The calculated rate constants for the FITC inactivation of ATPase (Figure 9A) and pNPPase (Figure 9A) activity were in the same range, when a single-exponential fit was applied. This indicates that the inhibition kinetics are similar in both cases and that a covalent modification of a single site by FITC is responsible for the loss of activity. Our results show that the inhibitory effect of FITC is found even with very small substrates such as *p*-nitrophenyl phosphate.

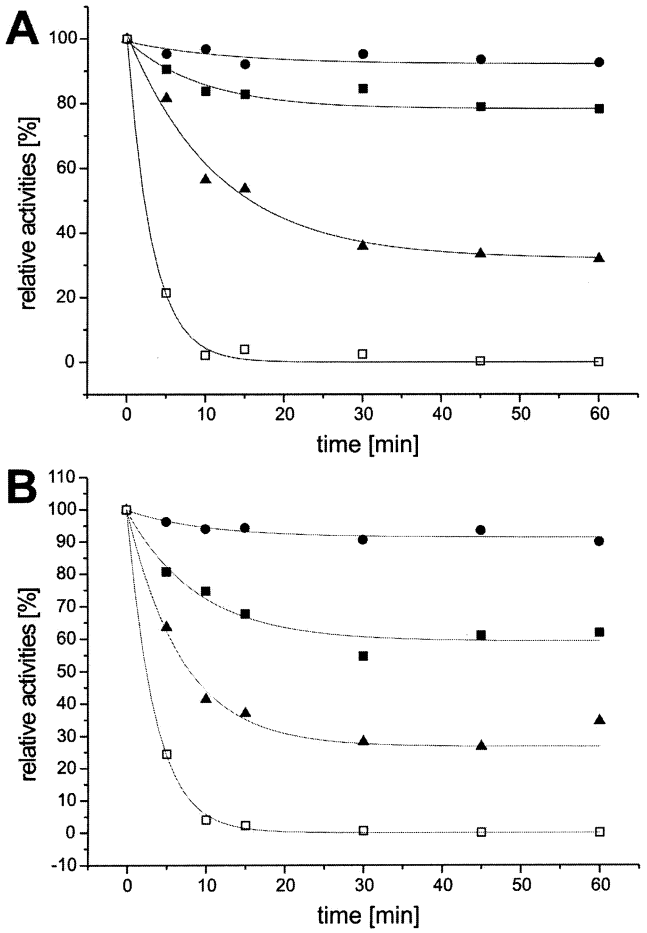

FIGURE 9: Inactivation of the ATPase (A) and pNPPase (B) activity of the Kdp-ATPase by FITC. The enzyme was incubated with various FITC concentrations at pH 9.2 and 37 °C. Samples were taken at different time points and subjected to gel filtration using NAP-5 columns equilibrated with 50 mM Tris-HCl (pH 8.0), 10 mM $MgCl_2$, and 0.2% aminoxide. The protein concentration of the eluate was determined. The same samples were used for the ATPase assay (A) with 10 μg/mL protein and for the pNPPase assay (B) with 50 μg/mL protein per reaction. The activities are indicated as percent values with an ATPase activity of 1350 μmol g^{-1} min^{-1} and a pNPPase activity of 51 μmol g^{-1} min^{-1} as 100% values. Data were fitted using a first-order exponential decay: (●) 0, (■) 50, (▲) 100, and (□) 250 μM FITC.

DISCUSSION

FITC modification at a lysine residue in the KGAPE motif of the Ca^{2+}-ATPase (SERCA1) (*16*), the Na^+,K^+-ATPase (*37*), the plasma membrane Ca^{2+}-ATPase (*56*), and the plasma membrane H^+-ATPase (*57*) abolishes the hydrolysis of ATP by these enzymes, but pNPP hydrolysis is retained. In contrast, both activities are affected by FITC modification in the case of the Kdp-ATPase. Sequence comparisons revealed that KdpB has a similar motif (395-KGSVD-399), and labeling of the KdpFABC complex with FITC in the presence of sodium or choline chloride revealed that of the four subunits only KdpB is labeled. Although the sequence analysis of the CNBr fragments does not prove that the KGSVD motif in KdpB is the binding site for FITC, the results at least confirm that the labeled fragments are part of the nucleotide-binding region of KdpB. These findings corroborate that FITC binds within the N-domain as found for other P-type ATPases. It is noteworthy that the Kdp-ATPase shares the FITC binding motif with the P-type ATPases of the type II−V classes (*1*), while the heavy metal-transporting ATPases lack this motif.

For the Na^+,K^+-ATPase, it was shown that ATP and ADP prevent FITC modification, while other nucleotides such as AMP and GTP had no effect (*42*). For the KdpFABC complex, we were able to demonstrate that not only ATP and ADP but, in contrast to the Na^+,K^+-ATPase, also AMP prevents FITC modification. Previously, it was reported that AMP is not or only binding with low affinity to recombinant nucleotide-binding domains of the Na^+,K^+-ATPase (*42*) and the Ca^{2+}-ATPase (*58*). However, it was reported that AMP binds with an apparent affinity of ~79 μM to the recombinant catalytic loop of the Wilson's disease protein (*59*). Since the size of the catalytic domains of the heavy metal-transporting ATPases and the Kdp-ATPase are similar, it seems that these smaller catalytic domains are less selective than their larger type II−V class counterparts. Furthermore, there is still discussion about the number of nucleotide-binding sites in a single polypeptide chain in P-type ATPases. Ward and Cavieres (*55*) proposed that a catalytic ATP binding site and a regulatory ATP binding site exist in the same molecule, while others believe that the two ATP binding sites are located on different subunits of a dimeric unit (*23*). Stokes and Green (*60*) suggested two possible cavities for ATP binding in the large cytoplasmic loop of the Ca^{2+}-ATPase by analyzing the 8 Å density map of the enzyme. Recently, experiments in which ADP was docked into a modeled nucleotide-binding domain of the Wilson's disease protein suggested the possibility of more than one nucleotide-binding site per protein chain (*61*). However, the binding of TNP-ATP to the Ca^{2+}-ATPase (*12*) and the solution structure of the N-domain of the Na^+,K^+-ATPase (*41*) make it most likely that only one binding site per catalytic subunit exists in P-type ATPases. The different behavior of the KdpFABC complex toward the protection of FITC labeling by nucleotides, namely, the prevention of FITC modification by AMP, might be due to high-affinity binding of AMP by the KdpFABC complex and the lack of discrimination between the different adenosine nucleotide phosphates. This high affinity for AMP is also reflected by the strong inhibition of pNPP hydrolysis by AMP. FITC-labeled enzymes of the Ca^{2+}-ATPase and the Na^+,K^+-ATPase still exhibit 80% of their pNPPase activity, while phosphorylation by ATP is completely abolished. FITC modifies the E1 and E2 conformations of the Ca^{2+}-ATPase (*18*). However, FITC inhibits only ATP-dependent partial reactions, whereas phosphorylation by P_i or Ca^{2+} uptake energized by acyl phosphate or pNPP was mainly retained (*18*). In the case of the KdpFABC complex, we could show that FITC labeling inhibits pNPPase activity with the same kinetics as the ATPase activity. Since sterical hindrance [access of larger substrates (e.g., ATP) is prevented, while hydrolysis of smaller ones (e.g., pNPP) is possible] is the basis for FITC inhibition, it seems most likely that in case of the KdpFABC complex the inhibition of the pNPP hydrolysis by FITC is due to the fact that this smaller substrate has no access to the nucleotide-binding site. This is strong evidence in favor of a much more compact structure of the catalytic loop (P- and N-domain) in the case of KdpB, compared to other P-type ATPases containing the FITC binding motif. Lysine 395, where FITC labeling most likely occurs, is so close to aspartate 307, the proposed phospho-

rylation site in KdpB (*25*), that even small substrates such as pNPP are sterically unable to bind after FITC binding. However, the FITC-modified KdpFABC complex exhibits differences compared to other P-type ATPases. Labeling of the complex inhibits the ATPase and pNPPase activity, which is termed the E1 ATP site and the E2 ATP site, respectively (*22*, *62*). Therefore, a simple explanation could be that FITC binds to both conformations of the ATP site. The existence of at least two nucleotide-binding sites in the active KdpFABC complex is also supported by the fact that ATP at lower concentrations stimulates the hydrolysis of pNPP. In conclusion, the KdpFABC complex could function as a dimer, where some ATP is needed to phosphorylate one monomer, which is then able to stimulate pNPP hydrolysis in the adjacent subunit. For the Na^+,K^+-ATPase, the oligomeric state is still a matter of controversy. However, evidence of a dimeric form (*23*, *63*) and evidence of the existence of more than one nucleotide-binding site per catalytic unit (*20*, *55*) have been presented. For the KdpFABC complex, the oligomeric state remains unclear. There are genetic data from cystronic complementation experiments which suggest at least a dimer as the functional unit of the KdpFABC complex (*64*). If this were the case, it would explain why higher ATP concentrations (>500 μM) inhibit pNPPase activity. At higher ATP concentrations, all ATP binding sites are occupied, and hence, pNPP is no longer hydrolyzed by the E2 site of the enzyme. If it is assumed that ATP binding accelerates the E2−E1 transition in the KdpFABC complex, it would explain the inhibition of pNPP hydrolysis. A similar conclusion has previously been reported for the Na^+,K^+-ATPase, where low concentrations of ATP also have a stimulating effect on pNPP hydrolysis while higher ATP concentrations were inhibitory (*70*). Indeed, there is some evidence that pNPP is only hydrolyzed in the E2 conformation. This is supported by the fact that *o*-vanadate is a strong inhibitor of this reaction. Vanadate is supposed to bind to the E2 conformation of P-type ATPases (*18*). The fact that the inhibition by vanadate is competitive with respect to pNPP strongly favors this view. The different inhibition kinetics of the ATPase activity might be related to the existence of two ATP binding sites. If it is assumed that the KdpFABC complex and other P-type ATPases possess two ATP binding sites, the biphasic behavior of both, ATP hydrolysis and its inhibition by *o*-vanadate, could easily be explained. On the basis of the assumption that the enzyme has a high-affinity ATP binding site that is accessible in the E1 state and a low-affinity ATP binding site that is exposed in the E2 state, different conditions for vanadate would exist. At low ATP concentrations, ATP will be bound predominantly to the high-affinity sites. The enzyme needs to be phosphorylated by ATP hydrolysis. The bottleneck of the reaction cycle may be the transition between E2 and E1 which means that most of the enzyme is in the E2-P form. After dephosphorylation, the binding of vanadate locks the enzyme in the E2 form. This cycle appears as uncompetitive inhibition since the substrate ATP has first to be bound and hydrolyzed and hence going along with increasing K_m and v_{max} values. Vashchenko *et al.* (*65*) reported an uncompetitive inhibition of the ATPase activity of the Ca^{2+}-ATPase by *o*-vanadate at high ATP concentrations ranging from 250 μM to 2 mM. At low ATP concentrations, the uncompetitive inhibition dominates with respect to the substrate ATP. At high ATP concentrations, the high-affinity binding site is saturated and the enzyme is in the steady state. The ATP is now competing competitively with vanadate since both the low-affinity ATP binding site and the binding of vanadate may occur in the E2 state. At this stage, the observed inhibition kinetics of vanadate are competitive with respect to substrates ATP and pNPP, since *o*-vanadate probably binds in the catalytic center and is, therefore, competing with pNPP as well. However, the nonlinear double-reciprocal plot in case of the Kdp-ATPase indicates the existence of more than one ATP site. A similar nonlinear effect of ATP hydrolysis is reported not only for P-type ATPases but also for the multidrug resistance transporter Mdr1, where a Lineweaver−Burk transformation of ATPase activity results in a nonlinear relation (*66*). For Mdr1, a cooperativity of at least four interacting sites was described (*66*).

It is interesting to note that in all cases reported so far, the transported ion has a severe effect on the pNPP hydrolysis and vanadate inhibition of P-type ATPases. This behavior is due to the fact that the transported ion binds to a specific conformational state and accelerates a change in conformation. In contrast to all P-type ATPases that have been identified, in the case of the Kdp-ATPase the potassium ion is transported by KdpA. Therefore, the "P-type" ATPase-like subunit KdpB might have no direct contact with the potassium ion while it is transported through KdpA. Another difference compared with other P-type ATPases is the relatively high basal ATPase activity of the Kdp-ATPase in the absence of potassium.

Finally, it can be concluded that the Kdp-ATPase shares similarities with the type II−V classes of P-type ATPases, as well as with the heavy metal-transporting ATPases. One can speculate whether the Kdp-ATPase is evolutionarily derived from the type II−V classes of P-type ATPases or if KdpB may be a kind of ancestor of the heavy metal-transporting ATPases. However, the existence of the FITC binding motif, and of seven putative transmembrane helices, and the size and sequence of the KdpB N-domain suggest that the Kdp-ATPase is more closely related to the H^+-ATPases (type III, according to ref *1*) and is therefore misgrouped as type Ia ATPase.

ACKNOWLEDGMENT

We are grateful to Dr. Roland Schmid for amino acid sequencing, Brigitte Herkenhoff-Hesselmann for excellent technical assistance, and Dr. G. Deckers-Hebestreit for constructive criticism.

REFERENCES

1. Axelsen, K. B., and Palmgren, M. G. (1998) Evolution of substrate specificities in the P-type ATPase superfamily, *J. Mol. Evol. 46*, 84−101.
2. Rhoads, D. B., Waters, F. B., and Epstein, W. (1976) Cation transport in *Escherichia coli*. VIII. Potassium transport mutants, *J. Gen. Physiol. 67*, 325−341.
3. Walderhaug, M. O., Polarek, J. W., Voelkner, P., Daniel, J. M., Hesse, J. E., Altendorf, K., and Epstein, W. (1992) KdpD and KdpE, proteins that control expression of the *kdpABC* operon, are members of the two-component sensor-effector class of regulators, *J. Bacteriol. 174*, 2152−2159.
4. Polarek, J. W., Williams, G., and Epstein, W. (1992) The products of the *kdpDE* operon are required for expression of the Kdp ATPase of *Escherichia coli*, *J. Bacteriol. 174*, 2145−2151.

5. Jung, K., and Altendorf, K. (2003) Stimulus perception and signal transduction by the KdpD/KdpE system of *Escherichia coli*, in *Regulatory networks in prokaryotes* (Dürre, P., and Friedrich, B., Eds.) pp 53−58, Horizon Scientific Press, Wymondham, U.K.
6. Siebers, A., and Altendorf, K. (1993) K^+-translocating Kdp-ATPases and other bacterial P-type ATPases, in *Alkali cation transport systems in prokaryotes* (Bakker, E. P., Ed.) pp 225−252, CRC Press, Boca Raton, FL.
7. Gassel, M., Möllenkamp, T., Puppe, W., and Altendorf K. (1999) The KdpF subunit is part of the K^+-translocating Kdp complex of *Escherichia coli* and is responsible for stabilization of the complex *in vitro*, *J. Biol. Chem. 274*, 37901−37907.
8. Durell, S. R., Bakker, E. P., and Guy, H. R. (2000) Does the KdpA subunit from the high affinity K^+-translocating P-type Kdp-ATPase have a structure similar to that of K^+ channels? *Biophys. J. 78*, 188−199.
9. Buurman, E. T., Kim, K. T., and Epstein, W. (1995) Genetic evidence for two sequentially occupied K^+ binding sites in the Kdp transport ATPase, *J. Biol. Chem. 270*, 6678−6685.
10. Gassel, M., and Altendorf, K. (2001) Analysis of KdpC of the K^+-transporting KdpFABC complex of *Escherichia coli*, *Eur. J. Biochem. 268*, 1772−1781.
11. Serrano, R. (1988) Structure and function of proton translocating ATPase in plasma membranes of plants and fungi, *Biochim. Biophys. Acta 947*, 1−28.
12. Toyoshima, C., Nakasako, M., Nomura, H., and Ogawa, H. (2000) Crystal structure of the calcium pump of sarcoplasmic reticulum at 2.6 Å resolution, *Nature 405*, 647−655.
13. Toyoshima, C., and Nomura, H. (2002) Structural changes in the calcium pump accompanying the dissociation of calcium, *Nature 418*, 605−611.
14. Aravind, L., Galperin, M. Y., and Koonin, E. V. (1998) The HD domain defines a new superfamily of metal-dependent phosphohydrolases, *Trends Biochem. Sci. 23*, 469−472.
15. Siebers, A., and Altendorf, K. (1989) Characterization of the phosphorylated intermediate of the K^+-translocating Kdp-ATPase from *Escherichia coli*, *J. Biol. Chem. 264*, 5831−5838.
16. Pick, U., and Bassilian, S. (1981) Modification of the ATP binding site of the Ca^{2+}-ATPase from sarcoplasmic reticulum by fluorescein isothiocyanate, *FEBS Lett. 123*, 127−130.
17. Carilli, C. T., Farley, R. A., Perlman, D. M., and Cantley, L. C. (1982) The active site structure of Na^+- and K^+-stimulated ATPase. Location of a specific fluorescein isothiocyanate reactive site, *J. Biol. Chem. 257*, 5601−5606.
18. Pick, U. (1981) Interaction of fluorescein isothiocyanate with nucleotide-binding sites of the Ca^{2+}-ATPase from sarcoplasmic reticulum, *Eur. J. Biochem. 121*, 187−195.
19. Rephaeli, A., Richards, D., and Karlish, S. J. (1986) Conformational transitions in fluorescein-labeled (Na,K)ATPase reconstituted into phospholipid vesicles, *J. Biol. Chem. 261*, 6248−6254.
20. Ward, D. G., and Cavieres, J. D. (1996) Binding of 2′(3′)-*O*-(2,4,6-trinitrophenyl) ADP to soluble α,β protomers of Na,K-ATPase modified with fluorescein isothiocyanate. Evidence for two distinct nucleotide sites, *J. Biol. Chem. 271*, 12317−12321.
21. Ward, D. G., and Cavieres, J. D. (1998) Photoinactivation of fluorescein isothiocyanate-modified Na,K-ATPase by 2′(3′)-*O*-(2,4,6-trinitrophenyl)8-azidoadenosine 5′-diphosphate. Abolition of E1 and E2 partial reactions by sequential block of high and low affinity nucleotide sites, *J. Biol. Chem. 273*, 14277−14284.
22. Linnertz, H., Thoenges, D., and Schoner, W. (1995) Na^+/K^+-ATPase with a blocked E1ATP site still allows backdoor phosphorylation of the E2ATP site, *Eur. J. Biochem. 232*, 420−424.
23. Linnertz, H., Urbanova, P., Obsil, T., Herman, P., Amler, E., and Schoner, W. (1998) Molecular distance measurements reveal an $(\alpha\beta)_2$ dimeric structure of Na^+/K^+-ATPase. High affinity ATP binding site and K^+-activated phosphatase reside on different α-subunits, *J. Biol. Chem. 273*, 28813−28821.
24. Puppe, W. (1991) Kalium-Transport bei *Escherichia coli*: Molekulargenetische und biochemische Untersuchungen zu funktionellen Domänen der Kdp-ATPase, Ph.D. Thesis, University of Osnabrueck, Osnabrueck, Germany.
25. Puppe, W., Siebers, A., and Altendorf, K. (1992) The phosphorylation site of the Kdp-ATPase of *Escherichia coli*: site-directed mutagenesis of the aspartic acid residues 300 and 307 of the KdpB subunit, *Mol. Microbiol. 6*, 3511−3520.
26. Siebers, A., and Altendorf, K. (1988) The K^+-translocating Kdp-ATPase from *Escherichia coli*. Purification, enzymatic properties and production of complex- and subunit-specific antisera, *Eur. J. Biochem. 178*, 131−140.
27. Siebers, A., Kollmann, R., Dirkes, G., and Altendorf, K. (1992) Rapid, high yield purification and characterization of the K^+-translocating Kdp-ATPase from *Escherichia coli*, *J. Biol. Chem. 267*, 12717−12721.
28. Fendler, K., Dröse, S., Altendorf, K., and Bamberg, E. (1996) Electrogenic K^+ transport by the Kdp-ATPase of *Escherichia coli*, *Biochemistry 35*, 8009−8017.
29. Völker, U., Engelmann, S., Maul, B., Riethdorf, S., Völker, A., Schmid, R., Mach, H., and Hecker, M. (1994) Analysis of the induction of general stress proteins of *Bacillus subtilis*, *Microbiology 140*, 741−752.
30. Antelmann, H., Bernhardt, J., Schmid, R., and Hecker, M. (1995) A gene at 333 degrees on the *Bacillus subtilis* chromosome encodes the newly identified sigma B-dependent general stress protein GspA, *J. Bacteriol. 177*, 3540−3545.
31. Hartree, E. F. (1972) Determination of protein: A modification of the Lowry method that gives a linear photometric response, *Anal. Biochem. 48*, 422−427.
32. Arnold, A., Wolf, H. V., Ackermann, B. P., and Baader, H. (1976) An automated continuous assay of membrane-bound and soluble ATPases and related enzymes, *Anal. Biochem. 71*, 209−213.
33. Laemmli, U. K. (1970) Cleavage of structural proteins during the assembly of the head of bacteriophage T4, *Nature 227*, 680−685.
34. Blum, H., Beier, H., and Gross, H. J. (1987) Improved silver staining of plant proteins, RNA and DNA in polyacrylamide gels, *Electrophoresis 8*, 93−99.
35. Weber, K., and Osborn, M. (1969) The reliability of molecular weight determinations by dodecyl sulfate-polyacrylamide gel electrophoresis, *J. Biol. Chem. 244*, 4406−4412.
36. Karlish, S. J. (1980) Characterization of conformational changes in (Na,K) ATPase labeled with fluorescein at the active site, *J. Bioenerg. Biomembr. 12*, 111−136.
37. Farley, R. A., Tran, C. M., Carilli, C. T., Hawke, D., and Shively, J. E. (1984) The amino acid sequence of a fluorescein-labeled peptide from the active site of (Na,K)-ATPase, *J. Biol. Chem. 259*, 9532−9535.
38. Tran, C. M., and Farley, R. A. (1986) Inhibition of ion pump ATPase activity by 3′-*O*-(4-benzoyl)benzoyl-ATP (BzATP): assessment of BzATP as an active site-directed probe, *Biochim. Biophys. Acta 860*, 9−14.
39. Adamo, H. P., Filoteo, A. G., and Penniston, J. T. (1996) The plasma membrane Ca^{2+} pump mutant lysine^{591}→arginine retains some activity, but is still inactivated by fluorescein isothiocyanate, *Biochem. J. 317*, 41−44.
40. Xu, K. (1989) Any of several lysines can react with 5′-isothiocyanatofluorescein to inactivate sodium and potassium ion activated adenosine triphosphatase, *Biochemistry 28*, 5764−5772.
41. Hilge, M., Siegal, W., Vuister, G. W., Güntert, P., Gloor, S. M., and Abrahams, J. P. (2003) ATP-induced conformational changes of the nucleotide-binding domain of Na,K-ATPase, *Nat. Struct. Biol. 10*, 468−474.
42. Gatto, C., Wang, A. X., and Kaplan, J. H. (1998) The M4M5 cytoplasmic loop of the Na,K-ATPase, overexpressed in *Escherichia coli*, binds nucleoside triphosphates with the same selectivity as the intact native protein, *J. Biol. Chem. 273*, 10578−10585.
43. Pick, U., and Karlish, S. J. D. (1980) Indications for an oligomeric structure and for conformational changes in sarcoplasmic reticulum Ca^{2+}-ATPase labelled selectively with fluorescein, *Biochim. Biophys. Acta 626*, 255−261.
44. Inesi, G. (1971) *p*-Nitrophenyl phosphate hydrolysis and calcium ion transport in fragmented sarcoplasmic reticulum, *Science 171*, 901−903.
45. Pucell, A., and Martonosi, A. (1971) Sarcoplasmic reticulum. XIV. Acetylphosphate and carbamylphosphate as energy sources for Ca^{2+} transport, *J. Biol. Chem. 246*, 3389−3397.
46. Nakamura, Y., and Tonomura, Y. (1978) Reaction mechanism of *p*-nitrophenyl phosphatase of sarcoplasmic reticulum. Evidence for two kinds of phosphorylated intermediates with and without bound *p*-nitrophenol, *J. Biochem. 83*, 571−583.
47. Rossi, B., de Assis Leone, F., Gache, C., and Lazdunski, M. (1979) Pseudosubstrates of the sarcoplasmic Ca^{2+}-ATPase as tools to study the coupling between substrate hydrolysis and Ca^{2+} transport, *J. Biol. Chem. 254*, 2302−2307.
48. Bodley, A. L., and Jencks, W. P. (1987) Acetyl phosphate as a substrate for the calcium ATPase of sarcoplasmic reticulum, *J. Biol. Chem. 262*, 13997−14004.

49. Jørgensen, P. L., Jørgensen, J. R., and Pedersen, P. A. (2001) Role of conserved TGDGVND-loop in Mg^{2+} binding, phosphorylation, and energy transfer in Na,K-ATPase, *J. Bioenerg. Biomembr. 33*, 367−377.
50. Ridder, I. S., and Dijkstra, B. W. (1999) Identification of the Mg^{2+}-binding site in the P-type ATPase and phosphatase members of the HAD (haloacid dehalogenase) superfamily by structural similarity to the response regulator protein CheY, *Biochem. J. 339*, 223−226.
51. Robinson, J. D., Levine, G. M., and Robinson, L. J. (1983) A model for the reaction pathways of the K^+-dependent phosphatase activity of the ($Na^+ + K^+$)-dependent ATPase, *Biochim. Biophys. Acta 731*, 406−414.
52. Fendler, K., Dröse, S., Epstein, W., Bamberg, E., and Altendorf, K. (1999) The Kdp-ATPase of *Escherichia coli* mediates an ATP-dependent, K^+-independent electrogenic partial reaction, *Biochemistry 38*, 1850−1856.
53. Scheiner-Bobis, G., Antonipillai, J., and Farley, R. A. (1993) Simultaneous binding of phosphate and TNP-ADP to FITC-modified Na^+,K^+-ATPase, *Biochemistry 32*, 9592−9599.
54. Mignaco, J. A., Barrabin, H., and Scofano, H. M. (1996) Effects of photo-oxidizing analogs of fluorescein on the sarcoplasmic reticulum Ca^{2+}-ATPase. Functional consequences for substrate hydrolysis and effects on the partial reactions of the hydrolytic cycle, *J. Biol. Chem. 271*, 18423−18430.
55. Ward, D. G., and Cavieres, J. D. (1998) Affinity labeling of two nucleotide sites on Na,K-ATPase using 2′(3′)-*O*-(2,4,6-trinitrophenyl)-8-azidoadenosine 5′-[α-^{32}P]diphosphate (TNP-8N_3-[α-^{32}P]-ADP) as a photoactivatable probe. Label incorporation before and after blocking the high affinity ATP site with fluorescein isothiocyanate, *J. Biol. Chem. 273*, 33759−33765.
56. Fioleto, A. G., Elwess, N. L., Enyedi, A., Caride, A., Aung, H. H., and Penniston, J. T. (1997) Plasma membrane Ca^{2+} pump in rat brain. Patterns of alternative splices seen by isoform-specific antibodies, *J. Biol. Chem. 272*, 23741−23747.
57. Pardo, J. P., and Slayman, C. W. (1988) The fluorescein isothiocyanate-binding site of the plasma-membrane H^+-ATPase of *Neurospora crassa*, *J. Biol. Chem. 263*, 18664−18668.
58. Moutin, M. J., Cuillel, M., Rapin, C., Miras, R., Anger, M., Lompre, A. M., and Dupont, Y. (1994) Measurements of ATP binding on the large cytoplasmic loop of the sarcoplasmic reticulum Ca^{2+}-ATPase overexpressed in *Escherichia coli*, *J. Biol. Chem. 269*, 11147−11154.
59. Tsivkovskii, R., MacArthur, B. C., and Lutsenko, S. (2001) The Lys1010-Lys1325 fragment of the Wilson's disease protein binds nucleotides and interacts with the N-terminal domain of this protein in a copper-dependent manner, *J. Biol. Chem. 276*, 2234−2242.
60. Stokes, D. L., and Green, N. M. (2000) Modeling a dehalogenase fold into the 8-Å density map for Ca^{2+}-ATPase defines a new domain structure, *Biophys. J. 78*, 1765−1776.
61. Lutsenko, S., Efremov, R. G., Tsivkovskii, R., and Walker, J. M. (2002) Human copper-transporting ATPase ATP7B (the Wilson's disease protein): biochemical properties and regulation, *J. Bioenerg. Biomembr. 34*, 351−362.
62. Hamer, E., and Schoner, W. (1993) Modification of the E_1ATP binding site of Na^+/K^+-ATPase by the chromium complex of adenosine 5′-(β,γ-methylene)triphosphate blocks the overall reaction but not the partial activities of the E_2 conformation, *Eur. J. Biochem. 213*, 743−748.
63. Thoenges, D., and Schoner, W. (1997) 2′-O-Dansyl analogs of ATP bind with high affinity to the low affinity ATP site of Na^+/K^+-ATPase and reveal the interaction of two ATP sites during catalysis, *J. Biol. Chem. 272*, 16315−16321.
64. Epstein, W., and Davies, M. (1970) Potassium-dependent mutants of *Escherichia coli* K-12, *J. Bacteriol. 101*, 836−843.
65. Vashchenko, V. I., Utegalieva, R. S., and Esyrev, O. V. (1991) Vanadate inhibition of ATP and *p*-nitrophenyl phosphate hydrolysis in the fragmented sarcoplasmic reticulum, *Biochim. Biophys. Acta 1079*, 8−14.
66. Buxbaum, E. (1999) Co-operating ATP sites in the multiple drug resistance transporter Mdr1, *Eur. J. Biochem. 265*, 54−63.
67. Lutsenko, S., and Kaplan, J. H. (1995) Organization of P-type ATPases: Significance of structural diversity, *Biochemistry 34*, 15607−15613.
68. Henkel, R. D., Van De Berg, J. L., and Walsh, R. A. (1988) A microassay for ATPase, *Anal. Biochem. 169*, 312−318.
69. Altendorf, K., Gassel, M., Puppe, W., Möllenkamp, T., Zeeck, A., Boddien, C., Fendler, K., Bamberg, E., and Dröse, S. (1998) Structure and function of the Kdp-ATPase of *Escherichia coli*, *Acta Physiol. Scand. 163*, 137−146.
70. Drapeau, P., and Blostein, R. (1980) Interactions of K^+ with (Na,K)-ATPase, *J. Biol. Chem. 255*, 7827−7834.

BI030198A